THE EFFECT OF INTRAUTERINE GROWTH RESTRICTION ON ATP CITRATE LYASE AND ELASTIN HISTONE ACETYLATION IN RAT LUNG

by

Sara Jane Shupe Fausett

A thesis submitted to the faculty of
The University of Utah
in partial fulfillment of the requirements for the degree of

Master of Science

in

Nutrition

College of Health

The University of Utah

August 2013

The University of Utah Graduate School

STATEMENT OF THESIS APPROVAL

The thesis of **Sara Jane Shupe Fausett**

has been approved by the following supervisory committee members:

Lisa A. Joss-Moore	, Chair	**04/19/2013**
E. Wayne Askew	, Member	**04/19/2013**
Kristine Jordan	, Member	**04/19/2013**

and by **E. Wayne Askew** , Chair of

the Division of **Nutrition**

and by Donna M. White, Interim Dean of The Graduate School.

ABSTRACT

Intrauterine growth restriction (IUGR) increases risk of neonatal lung disease. In animal models, the predisposition to neonatal lung disease is associated with a decrease in elastin production. Production of elastin is necessary for development of the lung. Cellular expression of elastin is encoded by the elastin gene. The expression of the elastin gene is modified by histone acetylation. Histone acetylation is made possible by the enzyme ATP-citrate lyase (ACL) in the nucleus, which provides Acetyl-CoA groups to acetylate histones. However, it is unknown whether IUGR is associated with changes in ACL mRNA and protein levels, global histone acetylation patterns, or elastin histone acetylation patterns. We hypothesize that IUGR will decrease ACL mRNA and protein levels and decrease global and elastin acetylation patterns. IUGR was induced by bilateral uterine artery ligation in Sprague Dawley rat dams at E19 of gestation. Lung tissue was collected from newborn control and IUGR rat offspring and ACL mRNA was quantified using real-time RT-PCR, ACL protein levels were quantified by Western blotting, global and elastin specific acetylation patterns were quantified using Western blotting and chromatin immunoprecipitation. Results are IUGR as % of sex matched control ± SD. IUGR decreased ACL mRNA levels in male and female IUGR rats (44 ± 8 and 75 ± 16, respectively) and ACL protein levels in male IUGR rats (32 ± 13). IUGR decreased ACL protein levels in the cytoplasm for males (92 ± 16) and in the nucleus for females (67 ± 25). Global histone acetylation patterns are decreased in males only (73 ± 13). Elastin specific acetylation patterns are decreased only in females (promoter 71 ± 13, exon 24 78 ± 16, and exon 33 48 ± 11). We conclude that IUGR sex specifically affects ACL mRNA and protein levels and global histone and elastin histone acetylation patterns in newborn rat lung. We speculate that, in female rat lung, decreased elastin is associated with decreased nuclear ACL protein levels.

To my loving husband and supportive family, thank you for all of your patience and love.

TABLE OF CONTENTS

LIST OF FIGURES

INTRODUCTION

Intrauterine Growth Restriction

Intrauterine growth restriction (IUGR) occurs when a fetus fails to achieve its genetic growth potential [1, 2]. IUGR is defined as an infant whose weight falls below the 10^{th} percentile for gestational age or by an alteration in umbilical blood flow [1, 2]. IUGR is the largest cause of fetal mortalities and morbidities, affecting 7-15% of pregnancies [1, 2]. IUGR can occur via compromised nutritional and/or endocrine environments in utero [1, 2]. Decreased nutrient flow to the fetus occurs due to placental insufficiency (UPI). The main cause of IUGR in developed countries is UPI, secondary to maternal hypertension [2].

IUGR increases the risk of preterm delivery and susceptibility to adult onset syndromes, disorders, and diseases [2-7]. **If the environment of the fetus is altered during critical periods of development for integral organs (i.e., heart, liver, lung), adaptive physiological alterations can occur.** The result of these adaptations often involves permanent alterations in gene expression resulting in physiological and developmental delays [3, 8].

IUGR and Lung Disease

Lung disease in IUGR is associated with delays in lung development [9, 10]. In humans, the final stage of lung development, alveolarization, occurs during fetal and early postnatal life [2, 4, 6, 7, 9, 11-14]. In rats, the species used for this study, alveolarization occurs entirely in the postnatal period. Postnatal alveolarization in rats and prenatal alveolarization in human infants encompasses the same relative degree of lung development. The immature rat makes a good comparison to the premature human lung without the complications of prematurity.

Premature IUGR infants have an increased incidence and severity of the chronic lung disease of infancy, bronchopulmonary dysplasia (BPD) [2, 4-6, 9, 11, 12, 14-17]. Human infants who died from BPD have alterations in lung structure. Structural changes to infant lungs are further exacerbated by mechanical ventilation and hyperoxia exposure [8, 9]. Hyperoxia and

mechanical ventilation increase distal parenchymal space and decrease elastin production in the lung, both of which negatively impacts the forming lung structure [1, 8-10, 18].

The developing lung requires appropriate nutrient availability to provide the necessary substrates for healthy tissue growth and differentiation. A decrease in nutrient supply, as occurs in UPI induced IUGR, causes alterations in lung function. In human and animal models, decreases in lung weight, alveolar cell maturation, and surfactant production are evident in IUGR lungs; changes that negatively impact the ability of the lung to develop properly [4-6, 11, 13, 15, 19]. In both human and animal models, UPI induced IUGR causes alterations in lung structure and impaired lung development [1, 2, 4-6, 9, 11-15, 17].

IUGR disrupts normal lung structure and development structure by numerous pathways, including elastin-dependent alveolar development [10].

Elastin

A key player in lung development is elastin. Elastin expression and processing is a primary factor in normal alveolar development as well as the formation and deposition of elastic fibers [10]. In normal mammalian development, elastin plays a critical role in lung development, namely: structural integrity and dispensability of airways, alveoli, extracellular matrix, and blood vessels [20]. Organization of lung elastin fibers starts in early lung development and peaks during alveolarization [21].

In animal models IUGR disrupts elastin expression and elastic fiber and lung tissue compliance [10, 22]. In mice, the deletion of the elastin gene leads to cardiorespiratory failure and death associated with reduced terminal airway branching and fewer distal air sacs [10, 20]. However, IUGR rats, who have decreased lung elastin expression, have lungs similar to control rats morphologically, but still exhibit decreased static lung compliance [10]. **We have shown in our IUGR model that elastin gene expression is reduced in newborn female rats, with male rats unaffected [23].** Decreases in elastin expression at birth increase susceptibility to lung complications and airway dysfunction later in life [10, 15, 19].

Elastin is encoded by the elastin (ELN) gene. The ELN gene consists of a single promoter and is 36 exons in length. Sequences of rat and human ELN genes are homologous with each other [10]. For humans and rats, appropriate elastin gene expression depends upon appropriate epigenetic regulation along the ELN gene [10, 24].

Epigenetics

Epigenetic modifications are heritable changes in gene transcription caused by mechanisms other than alterations in DNA sequence [5, 11, 12]. Such modifications consist of DNA methylation and histone protein phosphorylation, methylation, or acetylation. DNA methylation and histone protein modifications are impacted by environmental factors, such as: nutritional and/or endocrine restrictions [1, 3, 9, 17, 18].

In animal studies, IUGR causes epigenetic alterations in lung, brain, hepatic, and pancreatic tissues, impacting overall tissue functionality [3, 5, 6, 9, 17, 18, 25-32]. Furthermore, IUGR can induce increases or decreases in specific gene expression and regulation [1, 3, 9, 33, 34]. Our group has previously demonstrated that IUGR alters the epigenetic profile of several genes important to lung development and metabolism, including PPARγ, Setd8, and IGF-1 [1, 3, 9, 17, 18].

One component of the epigenetic profile is histone protein modifications (Figure 1A) [1, 9]. The structure of histones consists of two domains: 1) a globular domain that interacts with other histones and chromatin, the combination of DNA and histone proteins as they exist in the nucleus of eukaryotic cells, and 2) positively charged tails projecting from the globular domain that may bind to the negatively charged phosphate groups on DNA's backbone [23, 25]. Specifically, the tails of histone 3 and histone 4 are modified along the amino acid residues of the unstructured N-terminal tails (Figure 1B) [1]. Key to this study is the addition of an acetyl group on histone proteins, otherwise known as histone acetylation [2,13].

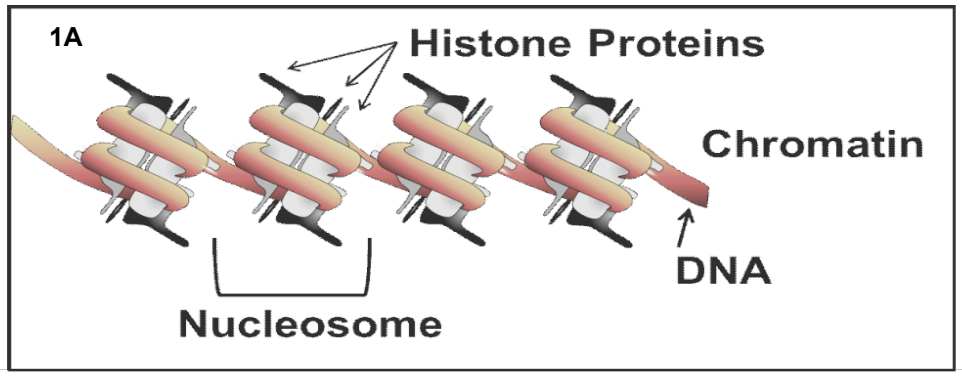

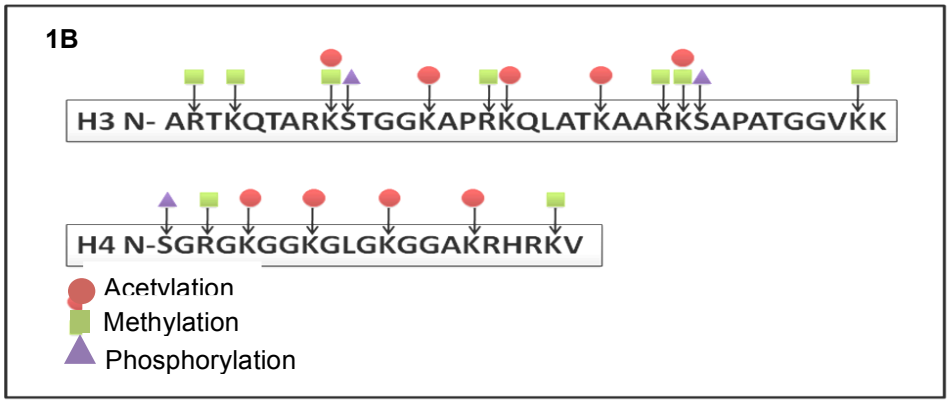

Figure 1: Chromatin structure and potential epigenetic modifications. 1A. Chromatin consists of DNA wrapped around a core of histone proteins, one unit of which is called a nucelosome. Epigenetic modifications include posttranslational modifications to N-terminal tails. One of the epigenetic modifications made to histone tails is acetylation [1]. 1B: The unstructured, N-terminal "tails" of the histone proteins are free to extend from the nucleosomes. Shown here are the H3 and H4 tails with potential modifications. Modifications occur on numerous amino acid residues simultaneously, providing a complex means of regulating transcription. The red circles indicate positions where histone acetylation takes place along histones 3 and 4 [1].

Histone Acetylation

Histone acetylation refers to the addition of acetyl groups to the positively charged histone tails [11, 12]. The acetylation process occurs via histone aceyltransferase (HAT) enzymes acting on lysine residues of the projecting histone tails [12, 25]. Modifications of these proteins can encode information on how genes are expressed by modifying the structure of the tails and, subsequently, the chromatin surrounding it [25]. The addition of an acetyl group destabilizes the chromatin binding to the histone tail by opening the chromatin conformation around the histone, increasing the incidence of transcription for many genes [12, 14, 25].

Acetylation and acetylation motifs play distinct roles in whole genome or single gene activity and transcription [35, 36]. Overall, acetylation has a multifactorial role in gene transcription, and the effects of acetylation depend upon both levels and location along the gene [35, 36]. In mammals, the acetyl groups for epigenetic modifications are produced primarily via citrate metabolism and the enzyme ATP Citrate Lyase (ACL) [1, 3, 4, 9, 17, 31, 33, 37, 38].

ATP Citrate Lyase

ATP Citrate Lyase (ACL) is an important intermediate in multiple metabolic processes (Figure 2) [31, 37, 38]. The best understood process occurs in the cytoplasm where ACL produces acetyl-CoA groups for lipid synthesis, important in surfactant production. A more recent discovery is that nuclear ACL produces the acetyl-CoA that is used to acetylate histones [32]. In nonlung tissue, it has been shown that ACL dependent acetyl-CoA contributes to increased histone acetylation during cellular response to growth factor stimulation as well as tissue differentiation [31]. Histone acetylation is dynamically regulated by physiologic alterations of ACL-produced acetyl-CoA [31].

In summary, we showed in our UPI-induced IUGR rat model that 1) IUGR changes lung structure in newborn female rats, not newborn male rats, 2) IUGR decreases elastin expression in newborn female rats, not newborn male rats, and 3) IUGR causes global changes in epigenetic modifications in the lung.

However, it is unknown if IUGR affects ACL levels or global and gene-specific acetylation of the ELN gene.

Hypothesis

UPI-induced IUGR will decrease ACL mRNA and protein levels in female newborn rat lung, without affecting male newborn rat lung. We further hypothesize that IUGR will decrease global histone 3 acetylation as well as acetylation along the elastin gene in newborn female rat lung.

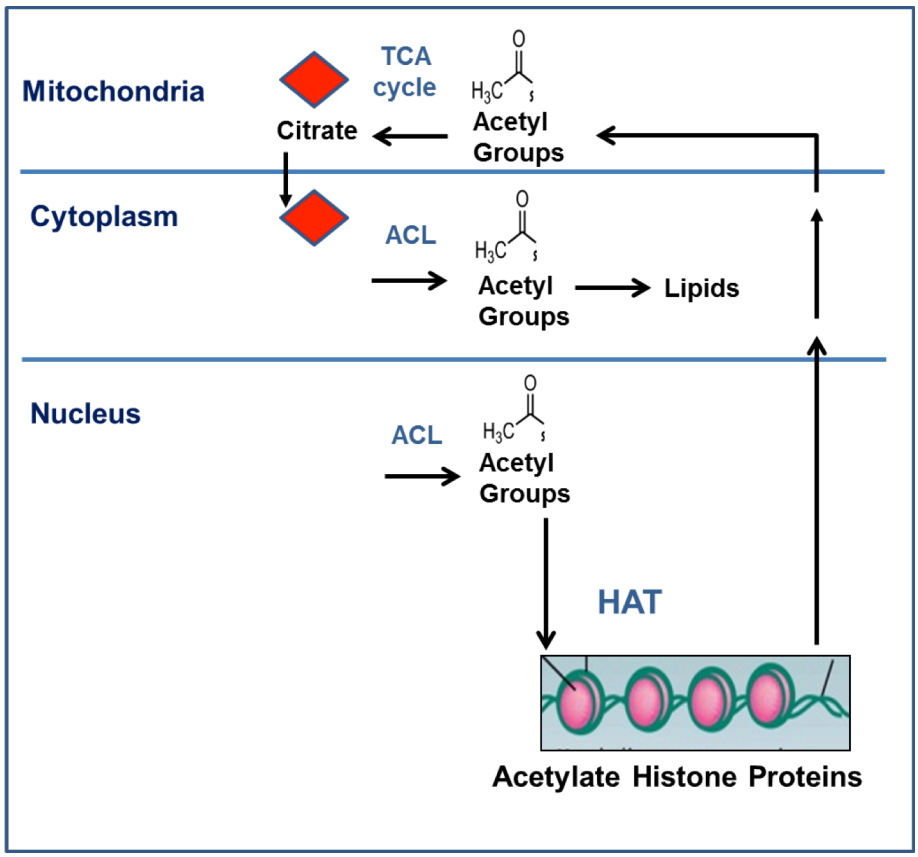

Figure 2: Cellular citrate, generated in the mitochondria is metabolized by the enzyme ATP citrate lyase (ACL) to produce Acetyl-CoA. In the cytoplasm, Acetyl-coA is used for subsequent lipid production. In the nucleus, acetyl CoA is used to produce the acetyl groups that are used to acetylate histones. Target genes include those which regulate glucose uptake and metabolism.

METHODS

Animals

Time-dated pregnant Sprague Dawley rats underwent bilateral uterine artery ligation on day 19 of a 21.5 day gestation to induce UPI and IUGR. On day 19, pregnant rats were anesthetized with intraperitonealxylazine (8mg/kg) and ketamine (40 mg/kg) [28]. Under sterile conditions, the abdomen was incised; the uterus isolated and removed from the abdominal cavity, and ligation of both the right and the left uterine arteries with a 3-0 silk suture [28, 30]. The uterus was then returned to the abdomen and incised closed with suture and wound clips. This procedure takes approximately 30 minutes and creates the IUGR environment [30]. Control dams were given the same anesthetization procedure. Arteries were not ligated on control dams.

At 2.5 days after bilateral uterine artery ligation, day 0 (d0) pups were delivered by caesarian section at term. D0 pups were sacrificed and whole lungs were harvested, flash-frozen with liquid nitrogen, and stored at -80^{0}C. Each experiment included 6 male and 6 female pups for each group (control and IUGR) [28]. To maximize variation from litter to litter, pups in each experimental group were derived from different litters. IUGR pups weighed approximately 25% less than control pups at birth [28, 30].

All procedures are in accordance to the American Physiological Society's guiding principles (2002) and were approved by the University of Utah Animal Care Committee [28].

Real-Time RT PCR

mRNA transcripts were measured in d0, control, and IUGR samples using real-time reverse transcriptase polymerase chain reaction (real-time RT-PCR). Real-time RT-PCR was used to evaluate mRNA abundance of ACL in lung tissue. Total RNA was extracted from frozen IUGR and control tissue using an RNeasy Plus Universal Midi Kit (Qiagen, DB Biosciences, CA) as per manufacturer protocol. RNA was then quantified using a NanoDrop 3300 Fluorospectrometer (Thermo Scientific, Wilmington, DE) and visualized by gel electrophoresis

[27]. An assay-on-demand primer and probe set was used for ACL, Rn0056641_m1 (Applied Biosystems, Carlsbad, CA). Levels for ACL mRNA were determined against GAPDH as an internal control (GAPDH primer and probe sequences: forward, CAAGATGGTGAAGGTCGGTGT; reverse, CAAGAGAAGGCAGCCCTGGT; probe, GCGTCCGATACGGCCAAATCCG) using the comparative Ct method [27]. All real-time RT-PCR amplification, data acquisition, and analysis were performed using the 7900HT Real-Time PCR system and SDS Enterprise Software (Applied Biosystems, Carlsbad, CA) with 384-Well Optical Reaction Plates (Applied Biosystems, Carlsbad, CA). Taqman Universal PCR Mastermix (Applied Biosystems, Carlsbad, CA) was used in a 5ul reaction [27]. Quadruplicates of each reaction were performed. Parameters for the cycle were: 50°C x 2 minute, 95°C x 10 minute, followed by 40 cycles of 95°C x 15 seconds, and 60°C x 60 seconds [27].

Protein Isolation and Western Blotting

Protein levels of ACL were measured in d0 control and IUGR lung tissue. Total protein was isolated by homogenization in RIPA buffer (50 mM Tris-HCL, Ph 8.0, 150 mM NaCl, 0.05% Na-deoxy-cholate, 1% NP-40 (Igepal), 0.1% SDS) and protease inhibitor cocktail (Applied Biosystems, Carlsbad, CA) [27]. Following homogenization, samples were centrifuged at 10,000g and 4°C for 15 minutes [27]. Supernatants were collected and assayed or stored at -80°C. Protein concentrations were assayed in triplicates using bicinchoninic acid protein assay kit (Pierce Biotechnology, Rockford, IL) [27].

Quantified protein samples were separated by 4-12% SDS-PAGE ready gels (Bio-Rad, Hercules, CA) and transferred to nitrocellulose membranes in standard transfer buffer (25mM Tris, 192 mM glycine, 20% methanol) [27]. Membranes were then blocked for 1 hour in 5% milk in Tris-buffered saline (TBS) [27]. Following blocking, membranes were exposed overnight at 4°C to rabbit polycolonal ATP Citrate Lyase Antibody (Cell Signaling Technology, Danvers, MA) at a 1:500 ratio. After extensive washing in TBS with 0.1% tween 20, a 1:5,000 dilution of antirabbit HRP secondary antibody (Cell Signaling Technology, Danvers, MA) was added and incubated for 1 hour at room temperature. Following extensive washing, signals were detected with Western

Lighting ECL (PerkinElmer Life Sciences, Boston, MA) and Biomax film (Amersham, Little Chalfont, UK) and quantified by Kodak Image Station 2000R (Eastman Kodak/ SIS, Rochester, NY) [27].

Separation of Nuclear and Cytoplasm Protein Compartments

Nuclear protein was isolated to provide substrate for compartmentalized Western blotting. Whole lungs were ground using liquid nitrogen and frozen at -80°C. Thawed tissue was resuspended in 400 µl of ice-cold buffer A (10 mM KCl, 10 mM HEPES, pH 7.9, 0.1 mM EDTA, pH 8.0, 1.0 mM DTT, 0.5 PMSF, and protease inhibitors) and incubated on ice for 15 minutes; followed by douncing with a loose pestle 20 times on ice and transferred into 1.5 ml tubes [27]. To separate the cytosolic and nuclear fractions, centrifugation was performed at 12,000g x 5 minutes at 4°C. The cytoplasmic supernatant was stored at -80°C [27]. The remaining tissue pellet was resuspended in 100 µl of ice-cold buffer C (1 mM DTT, 0.4 mM NaCl, 1.0 mM PMSF, 1.0 mM EDTA, 20 mM HEPES, pH 7.9, 0.5% NP-40, 1.0 mM EGTA, with glycerol 25% (vol/vol), plus protease inhibitors), incubated on a vortex rocker for 1.5 hours at 4°C, and centrifuged at 12,000g x 5 minutes at 4°C. Nuclear supernatants were aliquotted and assayed in triplicates using bicinchoninic acid protein assay kit (Pierce Biotechnology, Rockford, IL) [27].

Histone Isolation and Western Blotting

Global histone acetylation was measured by Western blotting. Histones were isolated from whole lung cells by acid extraction. Cells were harvested by centrifugation at 2,000g for 5 minutes at 4°C, washed in cold phosphate buffered saline (PBS), and resuspended in 1 ml of buffer A (20mm HEPES, pH 7.2, 1% sodium deoxycholate, 100mM NaCl, 50 mM NaF, 5 mM EDTA, 100 µM Na_2MoO_4, 1mM Na_3VO_4, 100 µM phenylmethylsulfonyl fluoride, 10 µg/ml leupeptin, 10 µg/ml aprotinin, 2 µg/ml pepstatin A, I mM benzamidine) [39]. Samples were then dounced for 20 strokes in a tight fitting glass/glass dounce homogenizer to produce lysates, followed by 3, 20-second pulses using a sonic dismembrator 100 (ThermoFisher, Waltham, MA) on ice [39]. Insoluble compounds were collected by centrifugation at 17,000g for 10 minutes, the pellets resuspended in buffer B (8m urea, 100 mM dithiothreitol, 1% Triton X-100), and incubated

for 10 minutes at room temperature [39]. After centrifugation at 17,000g for 10 minutes, the loose pellet was transferred to a new tube, and 1/10 of the existing volume of 0.3 nHCL was added [39]. Samples were then vortexed and incubated on ice for 30 minutes, followed by centrifugation at 13,000g for 10 minutes at 4°C [39]. Insoluble pellets were separated from the supernatant to a Side-A-Lyzer Mini Dialysis Unit and soaked in ddH_20 for 15 minutes 4°C to remove glycerol [39]. The addition of 300 ml 0.1 mM acetic acid and incubation overnight at -20°C precipitated histones and chromatin-associated proteins. The proteins were collected by centrifugation at 17,000g for 10 minutes and the pellets lyophilized and resuspended in 100 µl of 10 mM HEPES, pH 8.0, with protease inhibitors [39].

Histone concentrations were determined with a microbicinchoninic acid (BCA) protein assay kit (Pierce Biotechnology, Rockford, IL). Ten to 20 grams of isolated histones were separated on 4-12% MES SDS-PAGE gels with Coomassie staining to verify protein integrity and transferred by electroblotting to polyvinylidene difluoride membranes (Millipore Biotechnology, Billerica, MA) [29]. Blocking was performed in freshly prepared 5% bovine serum albumin (BSA) buffer. After washing, the membrane was incubated overnight at 4°C in BSA buffer with primary antibody: Anti-acetyl-Histone 3 antibody (Millipore Biotechnology, Billerica, MA) at a 1:1,000 ratio. Results were obtained from acetylated H3 and the same membrane was stripped with stripping buffer (62.5 mM Tris-HCL, pH 6.7, 2% SDS, 100 mM 2-mercaptoehtanol) at 55°C for 30 minutes and then reprobed with total H3 [29]. Secondary antibody was incubated for 1 hour at room temperature. A signal was detected with enhanced chemiluminescence (ECL) as per manufacturer's protocol (Amersham, Little Chalfont, UK) [29]. The amount of site-specific acetylated H3 was quantified relative to the amount of total H3 per sample [29].

Chromatin Immunoprecipitation

Acetylation along the elastin gene was measured by chromatin immunoprecipitation. Cell cross-linking was performed by adding 0.8 ml of 37% formaldehyde to 20 ml of overlaying media for 15 minutes, followed by 320 µl of 2M glycine to a final concentration of 0.125 M [40, 41]. Cells were then harvested and washed twice with 10 ml phosphate-buffered-saline (PBS). Cells were

then lysed with 1.0 ml IP buffer (150 mM NaCl, 5 mM EDTA, 1% Triton X-100, 0.5% NP-40, 50 mM Tris-HCl, pH 7.5, and 0.5 mM DTT) and a protease inhibitor cocktail (Roche Applied Science, Indianapolis, IN) [40, 41]. After one wash with 1.0 ml IP buffer the pellet was suspended in 1ml IP buffer and sheared by a sonicator microprobe for 7 rounds of 10, 10 second pulses at an output level of 10 (ThermoFisher, Waltham, MA) [40, 41]. After shearing, chromatin was centrifuged for 10 minutes at 17,000g, aliquotted, and stored at -80°C. Thawed chromatin was incubated for 30 minutes at room temperature in Anti-acetyl Histone H3 antibody (06599) (Millipore Biotechnology, Billerica, MA) with blocking peptide, then incubated in an ultrasonic water bath for 15 minutes at 4°C (Thermo Scientific, Wilmington, DE) [40, 41]. Tubes were then centrifuged at 17,000g for 10 minutes and the supernatant was placed in fresh tubes, followed with 20 µl of washed protein A magnetic beads (Cell Signaling Technology, Danvers, MA) [40, 41]. The slurry was rotated for 45 minutes at 4°C and the beads washed 5 times with 1 ml cold IP buffer containing no inhibitors [41].

At room temperature, 100 µl of 10% Chelex (10g/100 ml H_20) was directly added to washed protein A beads and vortexed, followed by boiling for 10 minutes and cooling to room temperature [40, 41]. Proteinase K (100 µl/ml) was then added and the beads incubated for 30 minutes at 55°C while shaking [41]. Tubes were then boiled again for 10 minutes. The suspension was centrifuged and supernatant collected [41]. The Chelex/protein A beads fraction was vortexed with 100 µl H_20, centrifuged again, and the supernatant collected and combined with the first [40, 41]. Eluate was then stored at -80°C for RT-PCR analysis.

Real-time RT-PCR was performed along the elastin (ELA) gene. Positions examined were: ELA promoter, exon 13, exon 17, exon 24, exon 25, exon 33, and 3' UTR. Primers and probes used are shown in Table 1, Figure 3. A nontranscribing intergenic region was used as the control [27].

Table 1
Primer/Probe sets for ChIP RT-PCR

Transcript position relative to the ELN gene	Sequence
Promoter	Forward: TTTGCCTGCAGATCTTGAACTC Reverse: GGGTTGGGTAGGTTGATGGA Probe: ATAGGCAGGCTCCCTT
Exon 17	Forward: CCAGCATCCCACCAGGAA Reverse: CAGGCTGGCCTTGAACCAT Probe: TGAGGTAGCAGGATTGATA
Exon 24	Forward: CCACCCTCATCGCTCTTCA Reverse: CTTCCAGAGCCCACCATGAT Probe: TGCCCAGAGAGGGAT
Exon 25	Forward: CTGGGAAGAGAACCCACAGTTC Reverse: GGGCAGGAGCTGTTGAAAAG Probe: TGACCCACTGAAGAC
Exon 33	Forward: CCCTCTCCAAAAGGCTTGTG Reverse: CACCATGAGCTGGGAAGATGT Probe: CTCCATCACCATGACC
3' UTR	Forward: GCTCCCCCACACAGTATCCA Reverse: AAGAAGAAGCACCAACATGTAGCCA Probe: CTCCAAGAGAAATTG

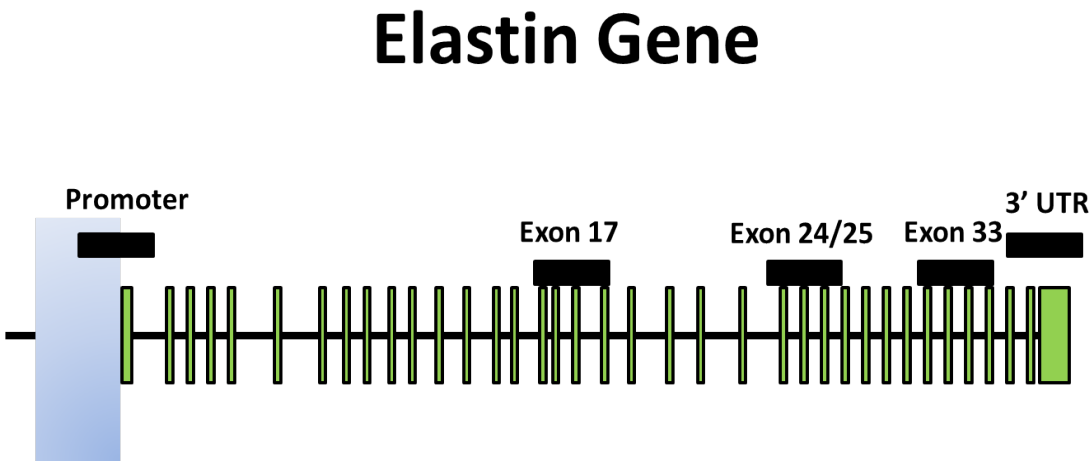

Figure 3: Structure of the elastin gene and positions investigated for changes in elastin acetylation. The promoter, exon 17, exon 24, exon 25, exon 33, and 3' UTR regions were chosen for investigation along the elastin gene because they started, were alternatively spliced, or finished elastin gene transcription.

Statistics

Data are presented as a mean ± SEM. IUGR data are presented as IUGR as percent of gender matched controls ± standard deviation (SD). Statistical differences between control and IUGR groups were determined using analysis of variance (ANOVA) and Mann-Whitney U nonparametric tests using the Statview software package (SAS Institute, Cary, NC). $P \leq 0.05$ was considered significant.

RESULTS

IUGR Decreases ACL mRNA In Male And Female Rat Lung

ACL mRNA transcript levels were quantified in newborn IUGR and control rat lungs via real-time RT-PCR. IUGR decreases ACL mRNA transcript levels in both male (p=0.012) and female (p=0.007) newborn rat lung relative to sex-matched controls (Figure 4).

IUGR Decreases ACL Total Protein Abundance In A Sex Specific Manner

Total ACL protein abundance was measured by Western blotting. IUGR decreases ACL protein abundance in males (p=0.017) but not in females (p=0.42) relative to sex-matched controls (Figure 5).

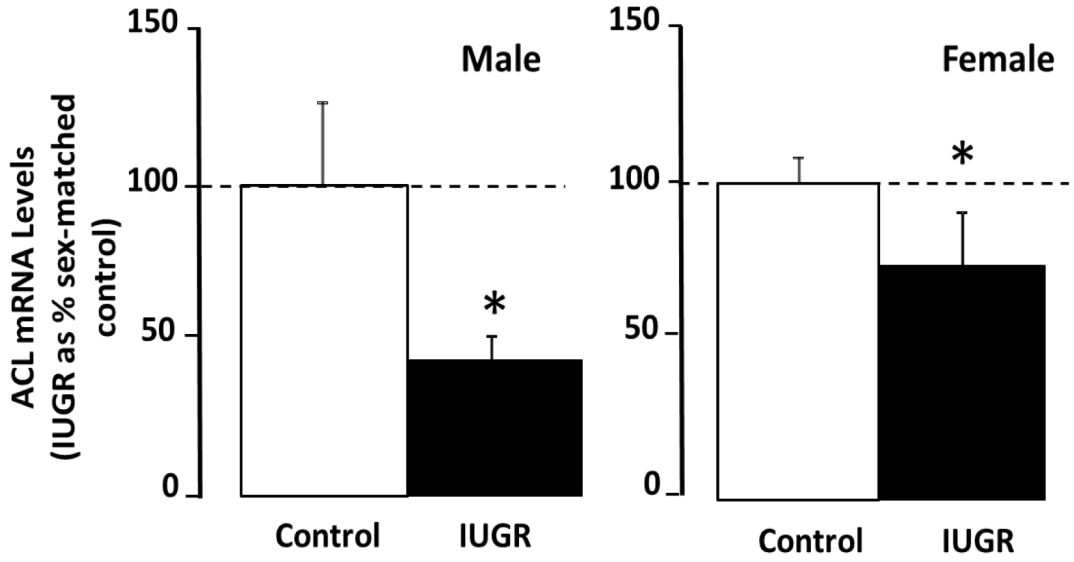

Figure 4: IUGR decreases ACL mRNA in male and female newborn rat lung. Compared to sex-matched controls, males and females have decreased ACL mRNA levels (p=0.012, p=0.007, respectively). Results are as IUGR as a percentage of sex-matched controls, where controls are normalized to 100%, shown by the dashed line. Error bars signify SD. Asterisks denote significant differences, n=6, *p≤.05.

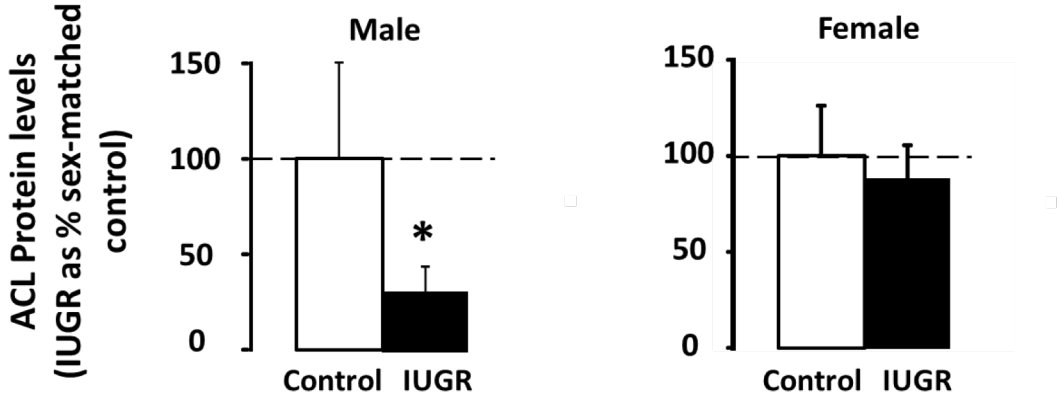

Figure 5: Upon IUGR insult, ACL protein levels are significantly decreased in males only (p=0.017). Results are as IUGR as a percentage of sex-matched controls, where controls are normalized to 100%, shown by the dashed line. Error bars signify SD. Asterisks denote significant differences, n=6, * p≤.05.

IUGR Alters ACL Protein Abundance In A Compartmentalized And Sex-Specific Manner

In an effort to determine compartment specific effects of IUGR on ACL protein levels, cytosolic and nuclear ACL protein concentrations were determined by Western blotting. In male rat lung, IUGR does not significantly affect ACL protein levels in the cytoplasm or nucleus compared to sex-matched controls (p=0.57 and p=0.13, respectively). In female rat lung, IUGR does not alter cytoplasmic ACL protein levels compared to sex-matched controls. However, in female rat lung, IUGR significantly decreases nuclear ACL protein levels compared to sex-matched controls (p=0.102 and p=0.047, respectively) (Figure 6).

IUGR Decreases Histone 3 Acetylation In Males

IUGR's effect on global histone acetylation was determined measuring whole lung H3 acetylation relative to total H3 via Western blotting. IUGR significantly reduces H3 acetylation in male (p=.03) newborn rat lungs, while no significant changes in female newborn rat lungs (p=.22) (Figure 7).

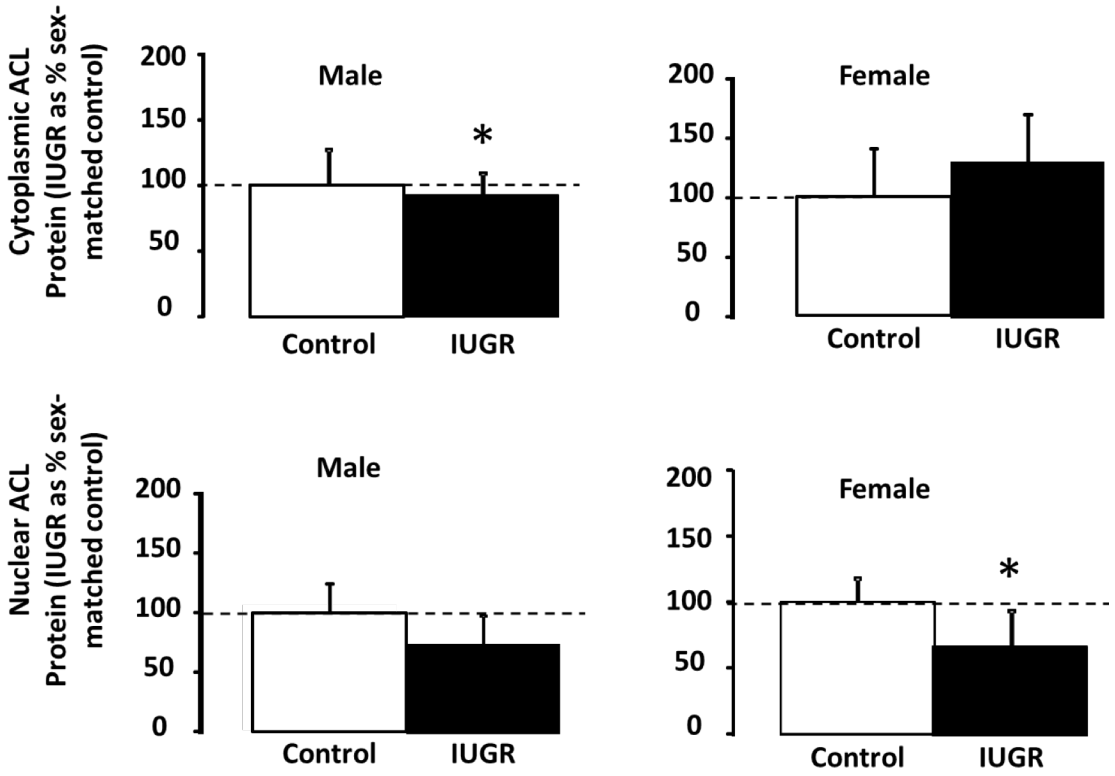

Figure 6: IUGR alters ACL protein levels in a cellular compartment- and sex-specific manner. In male IUGR rats there are no changes in ACL protein abundance in the cytoplasm or nucleus (p=0.57, p=0.13, respectively). Females only show a decrease in nuclear ACL protein abundance (p=0.46, p=0.046, respectively). Results are as IUGR as a percentage of sex-matched controls, where controls are normalized to 100%, shown by the dashed line. Error bars signify SD. Asterisks denote significant differences, n=6, * p≤.05.

IUGR Alters Acetylation Of The Elastin Gene In A Sex-Specific Pattern

In order to assess gene-specific acetylation we measured H3 acetylation at six positions along the elastin gene. We chose to examine the promoter, exon 17, exon 24, exon 25, exon 33, and the 3' UTR. We chose these positions as they represent locations were the elastin transcript is started, alternatively spliced, or finished (Figure 3). In male rat lung, compared to sex-matched controls, IUGR increases acetylation of the elastin gene in male rat lung at exon 17 (p=.016), exon 24 (p=.041), and the 3' UTR (p=.046). In female rat lung, IUGR decreases acetylation of the elastin gene at the promoter (p=.005), exon 1 (p=.046), and exon 24 (p=.016) (Figure 8).

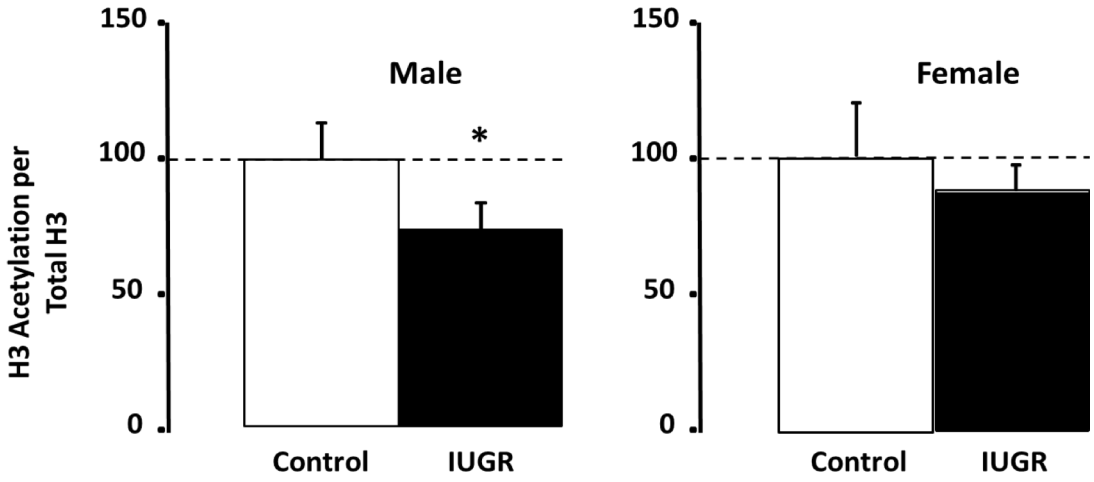

Figure 7: IUGR decreases H3 acetylation compared to total H3 in males (p=.03). Females show no decrease in total H3 acetylation (p=.22). Results are as IUGR as a percentage of sex-matched controls, where controls are normalized to 100%, shown by the dashed line. Error bars signify SD. Asterisks denote significant differences, n=6, * p≤.05.

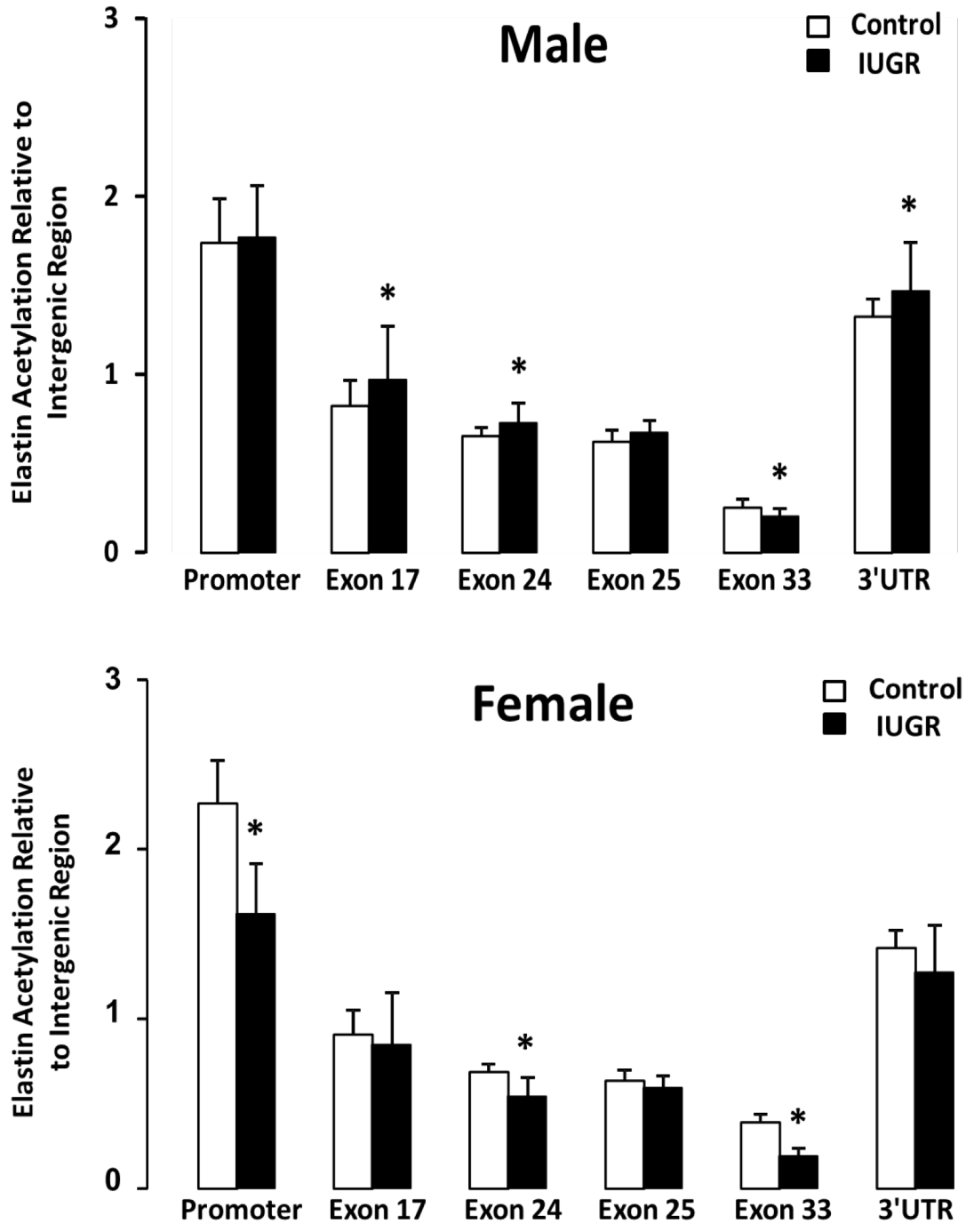

Figure 8: IUGR impacts acetylation of ELN expression in a sex-dependent manner. IUGR results are represented by black bars for both sexes. Controls are represented by white bars. Females show decreases of ELN at the promoter, exon 24, and exon 33 (p=0.005, p=0.016, p=0.00, respectively). Males show increases at exon 17, exon 24, and the 3' UTR (p=0.016, p=0.041, p=0.046, respectively). Interestingly, males also show a decrease at exon 33 (p=0.049). Asterisks denote significant differences, n=6, * p≤.05

DISCUSSION

Novel and important findings in this study are twofold. Firstly, IUGR decreases protein levels of the acetyl donor, ACL, in a compartment-specific and sex-specific manner in newborn rat lung. Secondly, IUGR alters gene-specific acetylation along the elastin gene in a sex-specific manner. Interestingly, in female rat lung, global acetylation is unchanged by IUGR, while elastin-specific acetylation is decreased. The IUGR-induced decrease in elastin acetylation, observed in this study is consistent with our previous observations of decreased elastin mRNA and altered structure in newborn female rat lung.

Sufficient ACL expression levels are necessary for mammals to survive [32]. Attempts to create an ACL knockout mouse are embryonic lethal, meaning that ACL is critical for survival [32]. ACL has two roles in the cell 1) cytoplasmic lipid production which is critical to lung function, and 2) nuclear acetylation of histones, which ultimately affects gene expression [30, 31, 32]. In order for ACL to function, glucose is required as substrate [30, 38]. However, glucose uptake is reduced in IUGR lung, due to decreased expression of genes transcribing for key metabolic enzymes [30, 38]. IUGR alterations in transcription of genes related to lung function have been shown previously by our lab [10, 27, 28, 42]. In our study, we show IUGR decreases ACL mRNA expression, which is consistent with previous studies linking glucose uptake and ACL expression (Figure 3) [38]. In our study, total ACL protein levels are reduced in male rat lung but not female rat lung. The discrepancy between reductions in total ACL mRNA expression and sex-specific total ACL protein levels promoted us to investigate cellular compartment ACL protein levels.

Results from cellular compartmentalized ACL protein levels show significant reductions in male IUGR cytoplasmic ACL protein levels, but not male IUGR nuclear protein levels. Interestingly, female IUGR rats show normal ACL protein levels in the cytoplasm, but decreases in the nucleus. We speculate that in male IUGR rats there is prioritization in maintaining nuclear ACL protein abundance levels over cytoplasmic levels, possibly to conserve histone modification [32]. Secondly, we speculate that female IUGR rats conserve cytoplasmic ACL protein levels to

maintain proper cytoplasmic and metabolic function at the expense of decreased nuclear histone modification. Furthermore, we suggest that female IUGR rats may be exhibiting increased ACL protein stability. In male lungs, nuclear ACL protein abundance was not significantly reduced, yet global acetylation was reduced. We speculate that failure to detect significant differences in ACL protein abundance in male IUGR rats may be due to an underpowered sample size or technical losses during nuclear extraction. Compartmentalized nuclear extracts require increased processing, leading to higher protein losses during extraction. Results from this study are novel, the differentiation between male IUGR and female IUGR ACL expression in the cytoplasm and the nucleus has not been previously characterized.

The activity of the ACL enzyme results in the production of acetyl-CoA groups which can be placed globally on histones and modify overall gene expression. The ability of ACL to provide acetyl-CoA groups for nuclear histone modification is measured indirectly by global histone acetylation [43]. Histone acetylation, activated by ACL in the nucleus, affects many important genes in lung structure and development [30, 38, 43]. In our study, global histone 3 acetylation in IUGR female rat lung did not decrease, despite decreases in ACL protein levels in the nucleus. Only IUGR male rats exhibit decreases in global histone 3 acetylation. However, global histone acetylation does not give any information about acetylation of target genes.

The detailed effects of IUGR on lung tissue by gene-specific acetylation patterns is generally not examined [1, 9, 10, 18]. In literature, global histone acetylation is frequently investigated. However, global histone acetylation tells little about gene-specific differences due to IUGR. Our lab has previously shown that IUGR affects numerous lung-specific gene targets, such as PPARy, Setd8, and ELN [10, 27, 42]. Our specific-gene target, elastin, is important for appropriate structure and development of lung tissue [10, 24, 44]. All segments of the ELN gene analyzed for IUGR acetylation modifications compared to sex-matched controls are shown in Figure 3. Interestingly, in female rat lung, where we have previously demonstrated a decrease in elastin mRNA levels, significant decreases in female ELN acetylation were seen at the promoter, exon 24, and exon 33. We speculate that the decreases in the acetylation of the promoter region

of the ELN gene with IUGR contribute to the previously observed decrease in elastin expression in female IUGR lungs.

Our results show the complexity of epigenetics and sex-specific and gene-specific acetylation. IUGR-induced changes in production by ACL, and placement of, acetyl-CoA for nuclear histone modification and gene expression is dependent upon sex and gene-specific targets. The newborn IUGR rats in our study show numerous sex-divergent affects which are supportive of previous research performed in our lab, indicating there are other factors effecting IUGR response other than the local organ system [23, 45]. Organ system alterations by IUGR may be due to differences in local tissue estrogen:testosterone ratio's, in male and female lungs [45]

This study utilizes a well-tested UPI model of IUGR, which creates asymmetrical growth restriction with a size reduction of 25% in IUGR rats compared to controls [27]. A rat model allows for larger control of confounding factors. However, the use of a rat model with a small sample size is the major limitation of our study, even though rat and human lung development are comparable. Experiments on rats limit our results to projections for future human studies.

In summary, IUGR affects 7-15% of pregnancies and epigenetically alters gene expression profiles of those neonates [1, 10, 15, 26, 28, 42]. Neonates with UPI-induced IUGR experience compromised nutrient flow, resulting in permanent alterations of ACL expression and elastin gene expression in rat lung tissue [1, 9, 10, 18]. Decreases in ACL expression may directly decrease lipid production in the cytoplasm, affecting surfactant levels. Altered surfactant levels increase the risk for bronchopulmonary dysplasia (BPD), which is aggravated by the use of mechanical ventilation [46]. Mechanical ventilation increases risk of BPD, especially in females due to poor surfactant production and structural alterations in lung tissue [46]. Further research may prove that, in order to prevent further structural alterations, different treatment options between male and female IUGR infants are utilized to decrease IUGR-induced BPD. IUGR-induced BPD impairs structure and function of lung tissue, predisposing IUGR infants to later lung dysfunction by alteration of lung structure and development possibly due to histone acetylation and elastin gene expression. Results and implications from this study offer further evidence of cellular

mechanisms for targeted interventions in decreasing IUGR's effects on lung tissue in neonates. In addition, the sex-divergent effects seen in IUGR females indicate there may be other influential factors in lung tissue development, such as systemic or local organ tissue environments and estrogen: testosterone ratios. IUGR permanently alters ACL expression and elastin gene profiles in male and female neonates. Results from this study provide further data regarding sex-divergent intervention targets to reduce adverse mechanistic, local, and global systemic effects in IUGR infants.

BIBLIOGRAPHY

1. Joss-Moore, L, Lane, RH. Perinatal nutrition, epigenetics, and disease. NeoReviews. 2011; 12:498-504.

2. Cetin, I, Alvino, G. Intrauterine growth restriction: implications for placental metabolism and transport. A review. Placenta. 2009;30:13.

3. Barker, DJ. Sir Richard Doll Lecture. Developmental origins of chronic disease: Public Health. 2012;126:185-9.

4. Harding, R, et al. The compromised intra-uterine environment: implications for future lung health. Clinical and Experimental Pharmacology and Physiology. 2000;27:965-74.

5. Lucas, JS, et al. Small size at birth and greater postnatal weight gain: relationships to diminished infant lung function. American Jouranl of Respiratory and Critical Care Medicine. 2004;170:534-40.

6. Maritz, GS, et al. Effects of fetal growth restriction on lung development before and after birth: a morphometric analysis. Pediatric Pulomonology. 2001;32:201-10.

7. Pallotto, EK, Kilbride, EW. Perinatal outcome and later implications of intrauterine growth restriction. Clinical Obstetrics and Gynecology. 2006;49:257-69.

8. West-Eberhard, MJ. Developmental Plasticity and Evolution 2003: Oxford University Press.

9. Joss-Moore, LA, Albertine, KH,Lane, RH. Epigenetics and the developmental origins of lung disease. Molecular Genetics and Metabolism. 2011;104:61-6.

10. Joss-Moore, LA, et al. IUGR decreases elastin mRNA expression in the developing rat lung and alters elastin content and lung compliance in the mature rat lung. Physiology and Genomics. 2011;43:499-505.

11. Alejandre Alcazar, MA, et al. Inhibition of TGF-beta signaling and decreased apoptosis in IUGR-associated lung disease in rats. PLoS One. 2011;6:20.

12. Doyle, LW, et al. Bronchopulmonary dysplasia in very low birth weight subjects and lung function in late adolescence. Pediatrics. 2006;118: 108-13.

13. Pike,KJ, Jane Pillow, J, Lucas, JS. Long term respiratory consequences of intrauterine growth restriction. Seminars of Fetal Neonatal Medicine. 2012;17:92-8.

14. Simmons, RA, et al. Intrauterine growth retardation: fetal glucose transport is diminished in lung but spared in brain. Pediatric Respiration. 1992;31:59-63.

15. Harding, R, Maritz, G. Maternal and fetal origins of lung disease in adulthood. Seminars of Fetal Neonatal Medicine. 2012;17:67-72.

16. Sato, Y, et al. Associations of intrauterine growth restriction with placental pathological factors, maternal factors and fetal factors; clinicopathological findings of 257 Japanese cases. Histololgy and Histopathology. 2013;28:127-32.

17. Wang, J, et al. Nutrition, epigenetics, and metabolic syndrome. Antioxidants and Redox Signaling. 2012;17:282-301.

18. Joss-Moore, LA, Lane, RH. The developmental origins of adult disease. Current Opinions in Pediatrics. 2009;21:230-4.

19. Huang, Y, et al. Hypoxia-inducible factor 2alpha plays a critical role in the formation of alveoli and surfactant. American Journal of Respiratory Cellular Molecular Biology. 2012;46:224-32.

20. Bland, RD, et al. Dysregulation of pulmonary elastin synthesis and assembly in preterm lambs with chronic lung disease. American Jouranl of Physiology and Lung Cellular Molecular Physiology. 2007;29:9.

21. Swee, MH, Parks, WC, Pierce, RA. Developmental regulation of elastin production. Expression of tropoelastin pre-mRNA persists after down-regulation of steady-state mRNA levels. Journal of Bioloigcal Chemistry. 1995;270:14899-906.

22. Lammers, SR, et al. Changes in the structure-function relationship of elastin and its impact on the proximal pulmonary arterial mechanics of hypertensive calves. American Journal of Physiology and Heart Circulcation Physiology. 2008;295:25.

23. Joss-Moore, LA, et al. Intrauterine growth restriction transiently delays alveolar formation and disrupts retinoic acid receptor expression in the lung of female rat pups. Pediatric Research. 2013;18:38.

24. Mithieux, SM, Weiss, AS. Elastin. Advanced Protein Chemistry. 2005;70:437-61.

25. Fu, Q, et al. Epigenetics: intrauterine growth retardation (IUGR) modifies the histone code along the rat hepatic IGF-1 gene. The FASEB Journal. 2009;23:2438-49.

26. Ke, X, et al. Intrauterine growth restriction affects hippocampal dual specificity phosphatase 5 gene expression and epigenetic characteristics. Physiological Genomics. 2011;43:1160-9.

27. Joss-Moore, LA, et al. Uteroplacental insufficiency increases visceral adiposity and visceral adipose PPARgamma2 expression in male rat offspring prior to the onset of obesity. Early Human Development. 2010;86: 179-85.

28. Joss-Moore, LA, et al. IUGR differentially alters MeCP2 expression and H3K9Me3 of the PPARgamma gene in male and female rat lungs during alveolarization. Birth Defects Research. Part A, Clinical and Molecular Teratology. 2011;91:672-81.

29. Ke, X, et al. Uteroplacental insufficiency affects epigenetic determinants of chromatin structure in brains of neonatal and juvenile IUGR rats. Physiological Genomics. 2006;25:16-28.

30. Ogata, ES, et al. Altered growth, hypoglycemia, hypoalaninemia, and ketonemia in the young rat: postnatal consequences of intrauterine growth retardation. Pediatric Research. 1985;19:32-7.

31. Wellen, KE, et al. ATP-citrate lyase links cellular metabolism to histone acetylation. Science. 2009;324:1076-80.

32. Chypre, M, Zaidi, N, Smans, K. ATP-citrate lyase: a mini-review. Biochemical Biophysiology Research Community. 2012;422:1-4.

33. Struhl, K, Histone Acetylation and transcriptional regulatory mechanisms. Genes and Development. 1998;12:599-606.

34. Voet, D, Voet, J, Pratt, W. Fundamentals of Biochemsitry: Life at the Molecular Level, 3rd Edition. 3rd edition. 2008, Wiley Press: United States. 1240.

35. Kurdistani, SK, Tavazoie, S, Grunstein, M. Mapping global histone acetylation patterns to gene expression. Cell. 2004;117:721-33.

36. Peterson, CL, Laniel, MA. Histones and histone modifications. Current Biology. 2004;14:R546-51.

37. Rathmell, JC,Newgard, CB. Biochemistry. A glucose-to-gene link. Science. 2009;324:1021-2.

38. Simmons, RA, Flozak, AS, Ogata, ES. Glucose regulates glut 1 function and expression in fetal rat lung and muscle in vitro. Endocrinology.1993;132: 2312-8.

39. Galasinski, SC, et al. Global regulation of post-translational modifications on core histones. Journal of Bioliogical Chemistry. 2002;277: 2579-88.

40. Kuo, MH, Allis, CD. In vivo cross-linking and immunoprecipitation for studying dynamic protein:DNA associations in a chromatin environment. Methods. 1999;19:425-33.

41. Nelson, JD, et al. Fast chromatin immunoprecipitation assay. Nucleic Acids Research. 2006:34.

42. Joss-Moore, LA, et al. IUGR decreases PPARgamma and SETD8 Expression in neonatal rat lung and these effects are ameliorated by maternal DHA supplementation. Early Human Development. 2010;86:785-91.

43. Cousins, RJ, Aydemir, TB, Lichten, LA. Plenary Lecture 2: Transcription factors, regulatory elements and nutrient-gene communication. Proceedings of the Nutrition Society. 2010;69:91-4.

44. Sechler, JL, et al. Elastin gene mutations in transgenic mice. Ciba Foundation Symposium. 1995;192:148-65.

45. Stiers JW, Yu, B, Callaway, C, Yu, X, Albertine, K, Lane, RH, Joss-Moore, LA. Intrauterine Growth Restriction alters mRNA Transcript Levels of Aromatase and Surfactant Protein in Neonatal Rat Lung. Journal of Investigative Medicine. 2013;61:123.

46. Sainz A, S.J., Wang, Y, Albertine, K, Lane, R, Joss-Moore, LA. Mild Neonatal Hyperoxia Exposure Decreases Lung Static Compliance in Male IUGR Rats. Journal of Investigative Medicine. 2013;61:123.